JCB Article

Endophilin B1 is required for the maintenance of mitochondrial morphology

Mariusz Karbowski, Seon-Yong Jeong, and Richard J. Youle

Biochemistry Section, Surgical Neurology Branch, National Institute of Neurological Disorders and Stroke, National Institutes of Health, Bethesda, MD 20892

We report that a fatty acyl transferase, endophilin B1, is required for maintenance of mitochondrial morphology. Down-regulation of this protein or overexpression of endophilin B1 lacking the NH_2-terminal lipid-modifying domain causes striking alterations of the mitochondrial distribution and morphology. Dissociation of the outer mitochondrial membrane compartment from that of the matrix, and formation of vesicles and tubules of outer mitochondrial membrane, was also observed in both endophilin B1 knockdown cells and after overexpression of the truncated protein, indicating that endophilin B1 is required for the regulation of the outer mitochondrial membrane dynamics. We also show that endophilin B1 translocates to the mitochondria during the synchronous remodeling of the mitochondrial network that has been described to occur during apoptosis. Double knockdown of endophilin B1 and Drp1 leads to a mitochondrial phenotype identical to that of the Drp1 single knockdown, a result consistent with Drp1 acting upstream of endophilin B1 in the maintenance of morphological dynamics of mitochondria.

Introduction

The dynamin family of large GTPases has been implicated in the regulation of membrane scission at several subcellular locations (Hinshaw, 2000; Praefcke and McMahon, 2004). The founding member of this family, the 100-kD GTPase dynamin, has been shown to participate in the vesicle scission step of clathrin-mediated endocytosis (Hinshaw, 2000; Praefcke and McMahon, 2004). Dynamin has been viewed as a mechanochemical enzyme that uses the energy released during GTP hydrolysis to pinch off constricted vesicles (Hinshaw, 2000; Praefcke and McMahon, 2004) or as a regulatory protein whose GTP-bound conformation allows recruitment of other effectors of vesicle scission (Sever et al., 2000). Additionally, several cofactors including the BAR (Bin-Amphiphysin-Rvs)-domain proteins, amphiphysin and endophilin I, are necessary for vesicle formation and completion of dynamin-mediated endocytosis (Hinshaw, 2000). It has been suggested that endophilin I may mediate changes in membrane curvature by enzymatic modification of the phospholipids in the bilayer membrane by transferring fatty acid groups to lysophosphatidic acid (Schmidt et al., 1999). Inhibition of endophilin I leads to formation of invaginated membrane intermediates that are arrested before vesicle constriction and scission, suggesting a critical role of this protein in the vesicle fission step (Gad et al., 2000; Huttner and Schmidt, 2000). Endophilin B1 (Farsad et al., 2001), also called SH3GLB1 (Pierrat et al., 2001) and Bif1 (Cuddeback et al., 2001), has been cloned and shown to have a domain organization and lipid tubulating activity similar to that of endophilin I (Farsad et al., 2001), although a role of this protein in membrane dynamics in vivo is not known.

Mitochondrial dynamics has been recently shown to be important for the normal function of the cell, including development of the sperm (Hales and Fuller, 1997), protection against ageing-related changes (Nakada et al., 2001), regulation of the Ca^{2+}signaling (Frieden et al., 2004), and progression of apoptosis (Frank et al., 2001). Several members of the dynamin protein family are essential for normal mitochondrial morphology. Dominant optic atrophy-associated protein (Opa1) and mitofusins 1 and 2 mediate fusion, whereas dynamin-related protein (Drp1) is required for division of these organelles (Mozdy and Shaw, 2003; Osteryoung and Nunnari, 2003). Although a requirement of these proteins for maintenance of the mitochondrial network has been established, their manner of action is not well understood. Several independent lines of evidence suggest that the mode of action of mitochondrial dynamin-like proteins resembles that of conventional dynamin. For example, like dynamin, Drp1 assem-

The online version of this article includes supplemental material.

Address correspondence to R.J. Youle, Bldg. 35, Rm. 917, MSC 3407, 35 Lincoln Dr., Bethesda, MD 20892-1414. Tel.: (301) 496-6628. Fax: (301) 402-0380. email: youler@ninds.nih.gov

Key words: endocytosis; LPAAT; dynamin; membrane tubulation; scission

Abbreviations used in this paper: AIF, apoptosis-inducing factor; IMM, inter mitochondrial membrane; OMM, outer mitochondrial membrane.

bles into multimeric ring-like structures in vitro under low salt conditions (Smirnova et al., 2001; Praefcke and McMahon, 2004) and Drp1 and dynamin have been shown to have membrane tubulation activity in vitro (Yoon et al., 2001; Praefcke and McMahon, 2004). Initiation and progression of the membrane events mediated by conventional dynamin involve the participation of accessory proteins (Hinshaw, 2000), and synchronous remodeling of the double membrane-bounded mitochondria may also require proteins in addition to components from the dynamin family. To date, genetic approaches in yeast have allowed the identification of several nondynamin proteins, which are required for the maintenance of mitochondrial morphology (Dimmer et al., 2002).

Here, we show that endophilin B1 is required for the maintenance of the normal mitochondrial morphology. We found that knockdown of endophilin B1 by RNAi leads to changes in mitochondrial shape, as well as the formation of outer mitochondrial membrane (OMM)–bound structures resembling those formed in neuronal terminals after inactivation of endophilin I. Our results indicate that Drp1 and endophilin B1 participate in distinct steps regulating dynamic stability of the mitochondrial network in mammalian cells and suggest more commonalities between the endocytosis and events occurring at the mitochondrial membranes than previously appreciated. Interestingly, it has been found that a homologue of endophilin B1, ERP1, has a role in the mitochondrial network maintenance in *Caenorhabditis elegans* (van der Bliek, A., personal communication), raising the possibility of a common, evolutionally conserved requirement of endophilin B1–like proteins in the mitochondrial morphology dynamics.

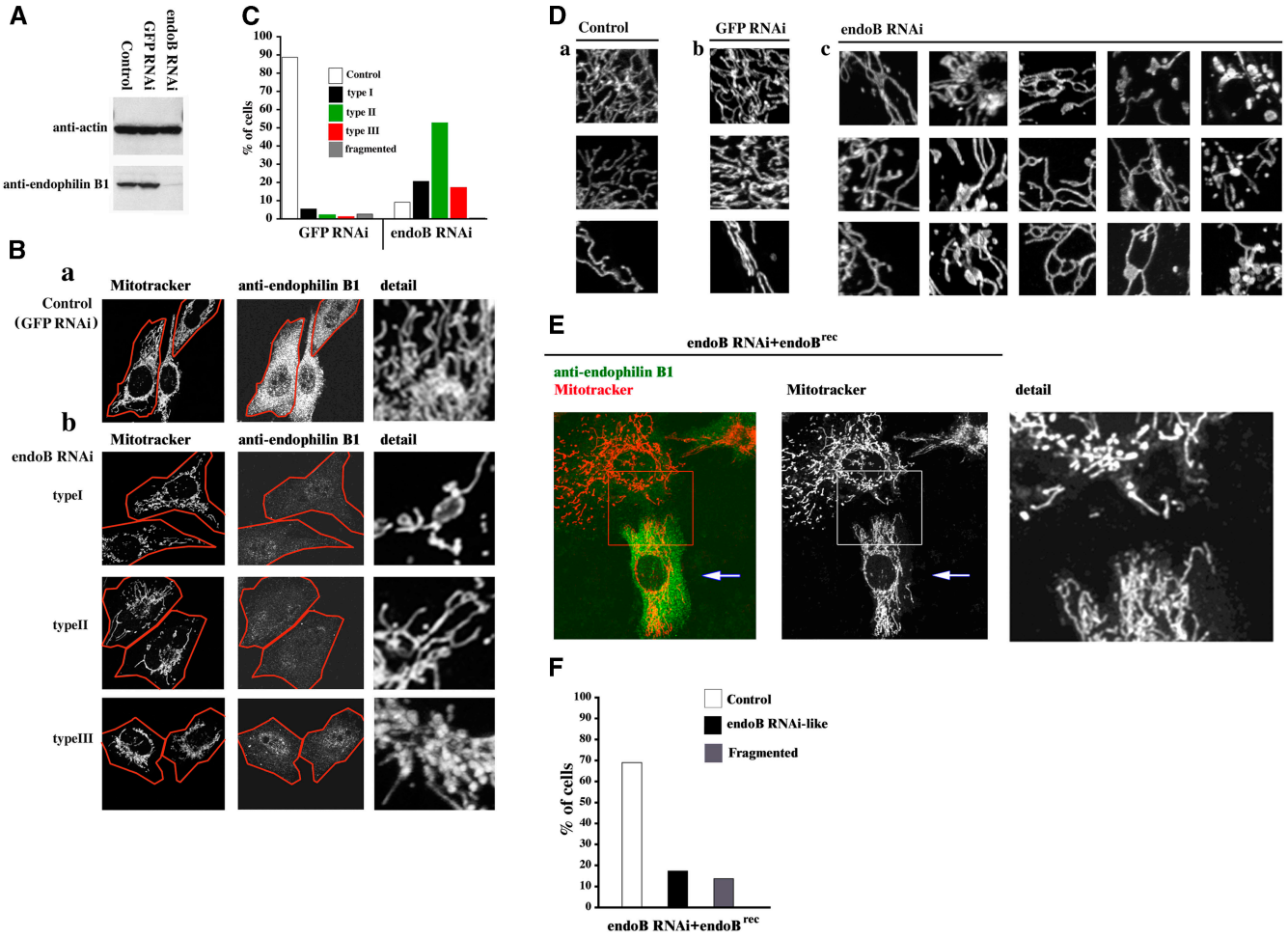

Figure 1. **Effects of endophilin B1 RNAi on mitochondrial morphology.** (A) Reduction of endophilin B1 levels after transfection with endoB RNAi vector. Control, hygromycin-resistant GFP RNAi, or endoB RNAi HeLa cells harvested 6 d after transfection with GFP- and endophilin B1–silencing vectors were analyzed for endophilin B1 by Western blotting. Actin was used as a loading control. (B) GFP RNAi (a) and endoB RNAi (b) cells were stained with Mitotracker and anti–endophilin B1 antibody and analyzed by confocal microscopy. Cells were divided into five groups based on the morphology of the mitochondrial network (see text). Representative images of four types are shown. (C) The percentage of GFP RNAi ($n = 531$) and endoB RNAi ($n = 417$) cells in each of five categories was scored. (D) Examples of mitochondrial network appearances in untransfected HeLa (a), GFP RNAi (b), and endoB RNAi (c) cells. Note the high diameter variability and unusual branching patterns of mitochondria in endoB RNAi cells. (E) Reconstitution of the mitochondrial phenotype in endoB RNAi cells by RNAi-insensitive mutant of endophilin B1. EndoB RNAi cells were transfected with a variant of endophilin B1 bearing five silent nucleotide substitutions located within a region targeted by RNAi construct. Cells were labeled with Mitotracker (red) and stained with anti–endophilin B1 mAbs (green). (F) Phenotypes of mitochondria in cells overexpressing endoB^{rec} construct (E, arrows) were scored ($n = 680$).

Results

Altered mitochondrial morphology and distribution in endophilin B1 RNAi cells

Endophilin B1 can directly interact with Bax (Cuddeback et al., 2001; Pierrat et al., 2001), a proapoptotic protein that has been shown to translocate to mitochondria and coalesce into foci colocalizing with the proteins known to regulate mitochondrial dynamics, Drp1 and Mfn2 (Karbowski et al., 2002). As mitochondrial activation of Bax is temporally linked to changes in OMM properties, as well as to the inhibition of the mitochondrial dynamics and mitochondrial fragmentation, we have speculated that endophilin B1 may participate in the regulation of the mitochondrial network maintenance (Karbowski and Youle, 2003).

To test this hypothesis, we constructed RNA silencing vectors using the short hairpin-activated gene-silencing system in which shRNAs are transcribed in vivo from a vector containing the human U6 promoter (pSHAG-1). To obtain selection of knockdown cells, shRNAs together with the U6 promoter were inserted into an episomal mammalian expression vector (pREP4) containing a hygromycin resistance selection marker. In HeLa cells transfected with pREP4-containing shRNA targeting an internal region of endophilin B1 and selected with hygromycin for 4–6 d (endoB RNAi cells), a dramatic reduction of the endophilin B1 protein expression level was achieved, whereas cells transfected with a green fluorescent protein–silencing construct (GFP RNAi cells) that has been used as a control RNAi in all experiments described in this paper were not affected (Fig. 1 A). To examine mitochondrial morphology, endoB RNAi, GFP RNAi, and untransfected HeLa cells were stained with a fluorescent marker of mitochondria, Mitotracker red CMXRos (Mitotracker), fixed, stained with anti–endophilin B1 mAbs, and analyzed by confocal microscopy. GFP RNAi cells (Fig. 1, Ba, C, and Db) have the characteristics of control nontransfected cells (Fig. 1 D), with an extended network of tubular mitochondria (~90%), of a fairly uniform tubule diameter of ~0.5–0.7 μm. In contrast, in endoB RNAi cells a distinct decrease in the expression of endophilin B1 was associated with alterations in mitochondrial morphology (Fig. 1, Bb, C, and Dc). In ~20% of endoB RNAi cells, misshaped, often unusually interconnected mitochondria, randomly distributed in the cytosol were detected (type I cells). About 50% of endoB RNAi cells contained a mixture of interconnected tubular and round mitochondria, mostly accumulating in the perinuclear area of the cells (type II cells). Certain cells (~20%) exhibited an apparent progression of the type II mitochondrial phenotype, with a further decrease of the mitochondrial tubule number and relocation of mitochondria to the perinuclear area associated with the formation of thick bleb-like structures (type III cells). In addition to the mitochondrial shape and distribution changes, endoB RNAi cells displayed a dramatic increase in the variability of the mitochondrial diameter (from ~0.5–0.7 to ~0.5–3.0 μm).

To exclude potential nonspecific effects of endoB RNAi, we inserted a mutant of endophilin B1 bearing five silent nucleotide substitutions, in the region targeted by the endoB RNAi construct, into the mammalian expression vector pcDNA3.1 (endoB^{rec}; see Materials and methods). EndoB RNAi cells were transfected with endoB^{rec}, followed by confocal microscopy analysis. In certain endoB RNAi cells transfected with endoB^{rec} an increase to the normal or above normal level of endophilin B1 expression was detected by immunostaining with anti–endophilin B1 mAbs, consistent with an efficient reconstitution of this protein (Fig. 1 E). Cells expressing levels of endoB^{rec} approximately the same as the normal level of endophilin B1 in control cells were used to quantify the effect of endophilin B1 reconstitution of the morphology of mitochondria. We found a distinct decrease in the number of the cells with aberrant mitochondria in endoB RNAi cells expressing endoB^{rec} (Fig. 1, E and F). These data indicate that the knockdown of endophilin B1 is responsible for the aberrant morphology of mitochondria in endoB RNAi cells.

It has been reported that the number, length, and tubular shape of mitochondria is a result of balanced fusion and fission rates (Mozdy and Shaw, 2003; Osteryoung and Nun-

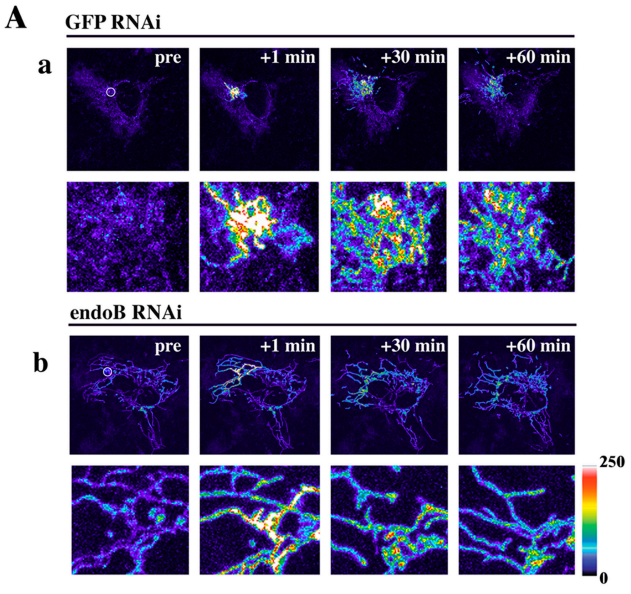

Figure 2. **Mitochondrial fusion rate is not affected by endophilin B1 knockdown.** Mitochondrial fusion rate was assayed using the mito-PAGFP–based mitochondrial fusion assay. (A) GFP RNAi cells (a) and endoB RNAi cells (b) were transfected with mito-PAGFP and assayed for mitochondrial fusion as described in Materials and methods. Pseudocolored images are used. (B) Changes in the fluorescence intensities of photoactivated mitochondria in GFP RNAi (a) and endoB RNAi (b) were measured over time.

nari, 2003). To address whether or not endoB RNAi affected mitochondrial fusion rates we applied a mitochondrial fusion assay based on measurements of dilution rates of the mitochondrial matrix-targeted photoactivable GFP (mito-PAGFP), as described previously (Karbowski et al., 2004). Mito-PAGFP–transfected GFP RNAi (Fig. 2, Aa and Ba) and endoB RNAi cells (Fig. 2, Ab and Bb) were analyzed over time after photoactivation of small clusters of mitochondria (Fig. 2, pre panels, white circles). A gradual decrease in the fluorescence of photoactivated mitochondria leading to the equilibrium between activated and nonactivated mitochondria is visible in both GFP RNAi ($t_{1/2}$[mito-PAGFP fluorescence decrease] = 35.5 ± 9.7; n = 20) and endoB RNAi ($t_{1/2}$[mito-PAGFP fluorescence decrease] = 34.9 ± 11.6; n = 32) cells, indicating that mitochondrial matrix fusion dynamics are not affected by knockdown of endophilin B1. We also analyzed the overall mitochondrial network remodeling dynamics by time-lapse confocal microscopy using endoB RNAi cells transfected with mito-YFP. Several of the abnormal mitochondria in these cells were found to retain the ability to change their shape and to convert from discoid, high-diameter structures, into tubular morphology (Video 1, available at http://www.jcb.org/cgi/content/full/jcb.200407046/DC1). Preserved fusion dynamics and an overall mitochondrial network plasticity, processes known to depend on the metabolic activity of mitochondria (Legros et al., 2002; Herlan et al., 2004), as well as an apparently normal accumulation of the vital probe $\Delta\Psi_m$-sensitive Mitotracker, suggest that mitochondrial shape defects in endoB RNAi cells are not due to metabolic incompetence of these organelles.

Knockdown of endophilin B1 does not affect the morphology of organelles other than mitochondria

We tested whether or not knockdown of endophilin B1 affects the subcellular distribution and morphology of membrane-bound organelles other than mitochondria. To detect the endoplasmic reticulum, GFP RNAi (Fig. 3 A) and endoB RNAi (Fig. 3 B) cells were stained with anti-BiP/GRP78 mAbs (Fig. 3, Aa and Ba) or transfected with endoplasmic reticulum retention signal tagged with DsRED2 (not depicted). Immunostaining with anti-GM130 (Fig. 3, Ab and Bb) or anti-GS28 mAbs (not depicted) was used for detection of the Golgi complex; anti-EEA1 mAbs (Fig. 3, Ac and Bc) and anti-Rab11 mAbs (Fig. 3, Ad and Bd) were used to detect early and recycling endosomes, respectively. Lysotracker red was applied to detect lysosomes (Fig. 3, Ae and Be). The morphology and distribution of peroxisomes was revealed by transfection with CFP-tagged peroxisome-targeting sequence (Fig. 3, Af and Bf). Confocal microscopy analyses revealed a lack of any visible changes of these analyzed organelles in endoB RNAi compared with GFP RNAi cells, indicating that mitochondrial defects in endoB RNAi cells may neither be the result of, nor are associated with, morphological changes in these other membrane-bound organelles. As the intracellular transport of mitochondria depends on microtubules (Nangaku et al., 1994), we also tested the effect of endophilin B1 down-regulation on the distribution of α-tubulin. We did not observe any visible differences in microtubule morphology between control, GFP RNAi, and endoB RNAi cells (unpublished data).

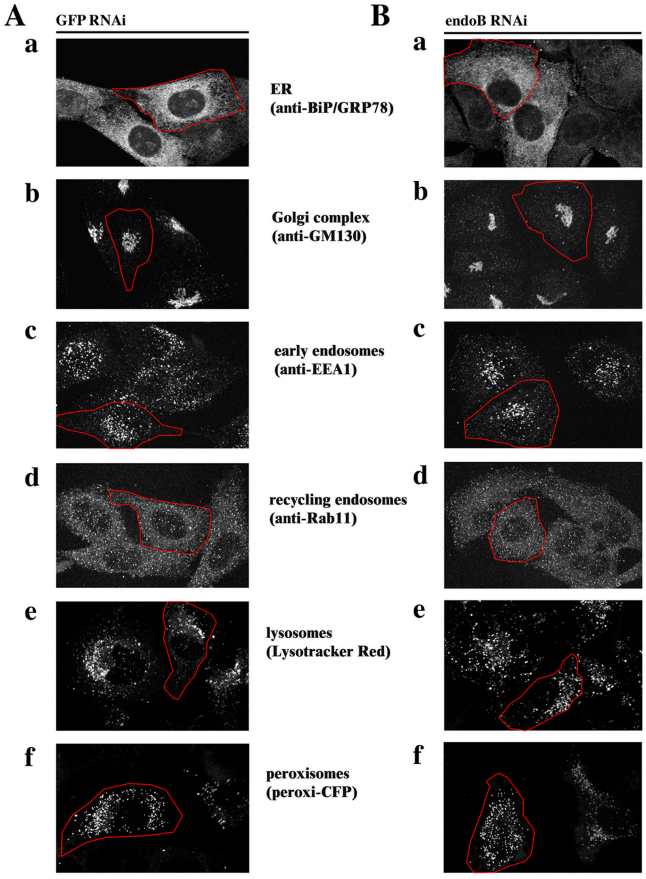

Figure 3. **EndoB RNAi does not affect the morphology of membrane-bound organelles other than mitochondria.** Morphology of ER (Aa and Ba), Golgi complex (Ab and Bb), early endosomes (Ac and Bc), recycling endosomes (Ad and Bd), lysosomes (Ae and Be), and peroxisomes (Af and Bf) in GFP RNAi (A) and endoB RNAi cells (B) was analyzed by confocal microscopy. Representative images are shown.

Dissociation of OMM and inter mitochondrial membrane (IMM) compartments in endoB RNAi cells

Because endophilin B1 homologues participate in membrane remodeling events at different subcellular locations (Huttner and Schmidt, 2000; Habermann, 2004) and activation of the endophilin B1 binding partner Bax has been described to affect OMM integrity (Degli Esposti and Dive, 2003), we asked if endophilin B1 is also required for OMM dynamics. The morphology of OMM and IMM compartments in GFP RNAi and endoB RNAi cells was analyzed simultaneously. Cells were stained with Mitotracker followed by immunolabeling with antibodies recognizing two proteins resident in the mitochondrial intermembrane space: (1) cytochrome *c* (Fig. 4, A and B) and (2) apoptosis-inducing factor (AIF; not depicted). As in control HeLa cells (not depicted), the Mitotracker staining pattern in GFP RNAi cells completely colocalized with cytochrome *c* (Fig. 4 A) and AIF (not depicted). However, in several endoB RNAi cells, numerous vesicular structures continuous with the mitochondria were stained with anti–cytochrome *c* (Fig. 4 B, blue arrowheads), and anti-AIF (not depicted) antibodies, but not with Mitotracker, indicating a separation of the OMM and IMM compartments and suggesting that the activity of endophilin B1 is required for the maintenance of

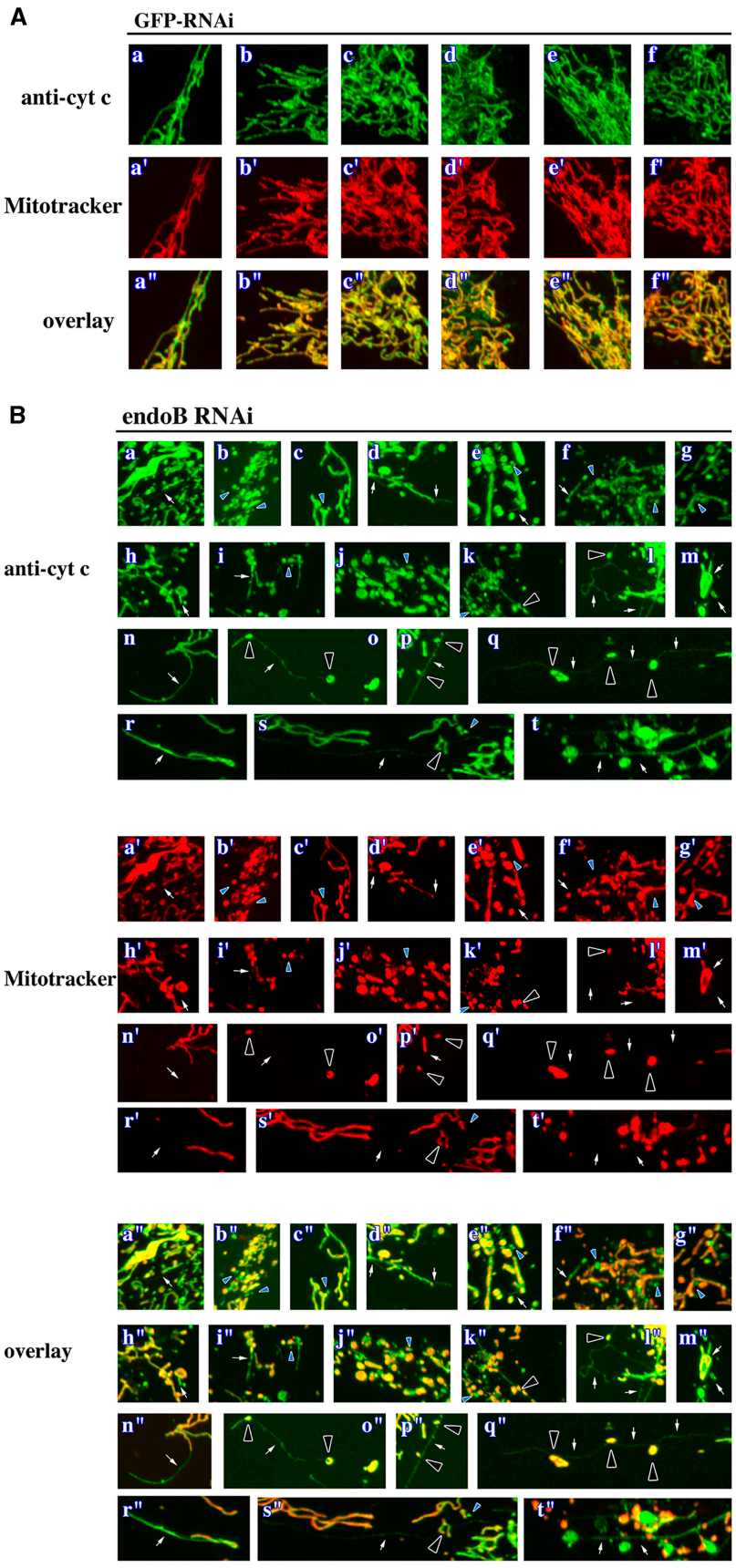

Figure 4. **Dissociation of OMM and IMM compartments in endophilin B1–depleted cells.** GFP RNAi (A and C) and endoB RNAi (B and D) cells were labeled with Mitotracker (A, a′–f′; and B, a′–t′) or transfected with mito-DsRED2 (C, a′–f′; and D, a′–j′) to reveal the mitochondrial matrix compartment, and stained with anti–cytochrome *c* mAbs (A, a–f; and B, a–t) or transfected with YFP-Fis1 (C, a–f; and D, a–j) to reveal the OMM compartment. Representative images are shown. Note the complete colocalization of matrix and OMM compartments in GFP RNAi cells and the formation of isolated OMM compartments in endoB RNAi cells (examples are indicated by arrows). In several cases, retracted matrix compartments (arrowheads) were located along, and connected by, thin tubules of OMM. (E) Drp1 in HeLa cells was depleted using pREP4-Drp1 RNAi system (see Materials and methods). Control HeLa cells or cells transfected with GFP RNAi or Drp1 RNAi that were selected with hygromycin for 4 d were analyzed by Western blot for Drp1 levels. Actin was used as a loading control. (F) Drp1 RNAi cells were stained with Mitotracker and anti–cytochrome *c* mAbs and analyzed by confocal microscopy. Note the high level of connectivity of mitochondria and the complete colocalization of IMM- and OMM-enveloped compartments.

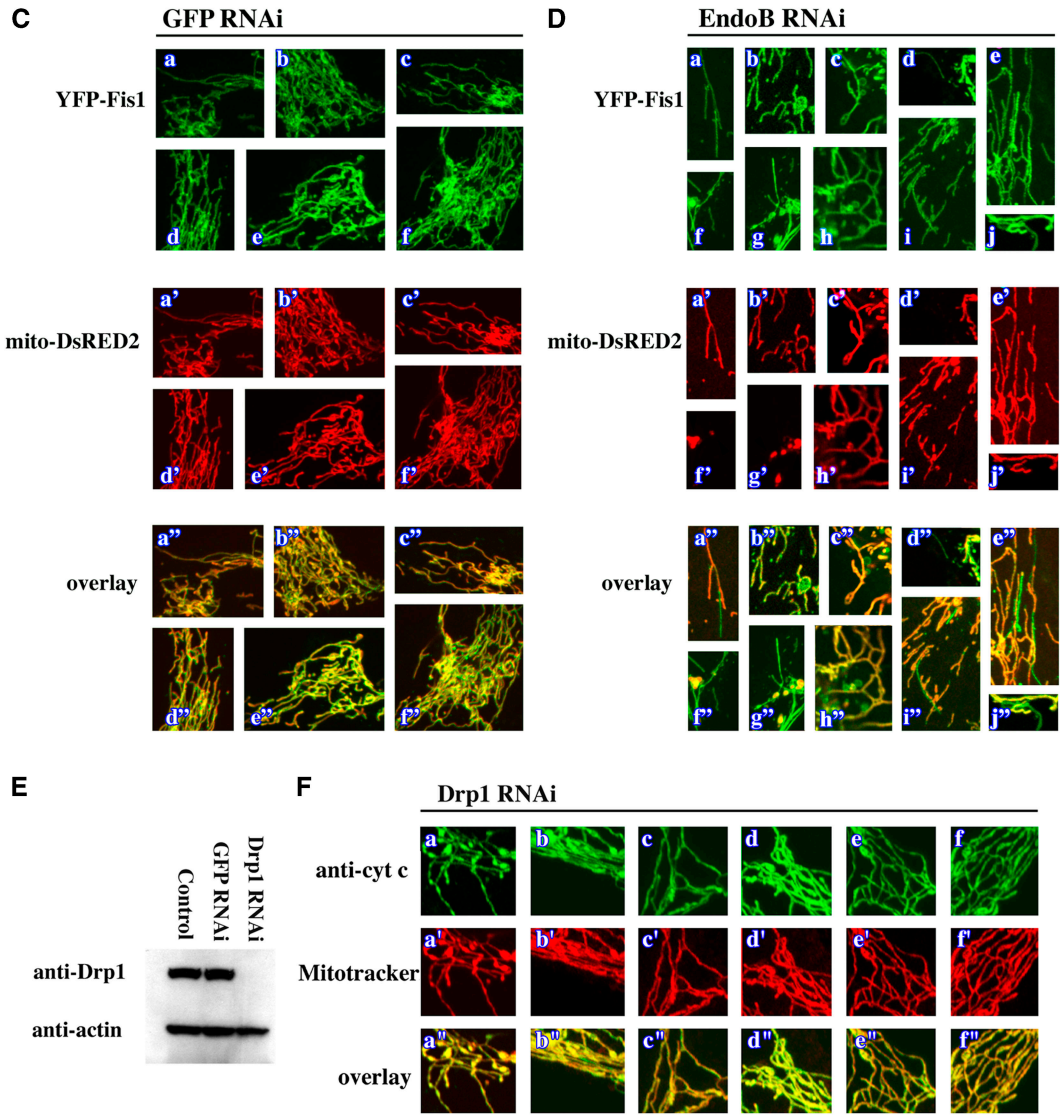

Figure 4 (continued)

OMM and IMM synchrony. Certain endoB RNAi cells also displayed, in addition to the aberrant vesicular OMM structures, OMM tubules emanating from the matrix varying in length from 2 μm to several tens of micrometers and diameters from 0.1–2.0 μm (Fig. 4, B, white arrows, and D). In extreme cases, the retracted matrix compartment formed beadlike structures located along and connected by thin tubules of OMM compartment (Fig. 4, B, black arrowheads, and D). We also analyzed the matrix and OMM synchrony in GFP RNAi and endoB RNAi cells cotransfected with another marker of the mitochondrial matrix, mito-DsRED2, and a YFP-tagged integral protein of the OMM, Fis1 (YFP-Fis1). Although high expression levels of a similar GFP-Fis1 construct have been reported to induce perinuclear clustering of mitochondria (Yoon et al., 2003), overexpression of low or moderate levels of YFP-Fis1 in HeLa cells does not alter mitochondrial morphology (Fig. 4 C). Because it has been also shown that fluorescent protein-tagged Fis1 localizes exclusively to the OMM (Yoon et al., 2003), we used it as a fluorescent marker of this compartment. Separation of the OMM from the matrix compartment was detectable in several endoB RNAi cells expressing mito-DsRED2 and YFP-Fis1 (Fig. 4 D), but not in the GFP RNAi cells (Fig. 4 C), confirming a dissociation of OMM and IMM dynamics in endoB RNAi cells. Moreover, separation of the OMM compartment from that of the matrix was also confirmed with fluorescence loss in photobleaching experiments (unpublished data). These data indicate that endophilin B1 may function selectively on the OMM and that the changes of the matrix compartment in endoB RNAi cells may be secondary to direct OMM defects.

Because down-regulation of *C. elegans* Drp1, a protein required for the division of mitochondria, led to a dissociation of the OMM compartment from the mitochondrial matrix (Labrousse et al., 1999), we also analyzed matrix and OMM compartment colocalization in Drp1 RNAi HeLa cells. Cells transfected with a pREP4 vector containing a Drp1 silencing sequence were selected with hygromycin for 4–6 d and analyzed by Western blotting for Drp1 (Fig. 4 E) and for mitochondrial morphology by costaining

with Mitotracker and anti–cytochrome *c* antibodies (Fig. 4 F). A decrease of Drp1 expression in Drp1 RNAi cells was, as already reported (Labrousse et al., 1999; Smirnova et al., 2001), associated with elongation and increased interconnection of mitochondria. Unlike in Drp1 RNAi *C. elegans* muscle and endoB RNAi HeLa cells (Fig. 2), Drp1 RNAi cells show complete colocalization of the matrix and the OMM, suggesting that divergent mechanisms may govern mitochondrial scission and OMM/IMM coupling in *C. elegans* and mammals.

Overexpression of endophilin B1 lacking the NH_2-terminal, amphipathic domain induces mitochondrial morphology defects and dissociation of OMM and IMM compartments

It has been shown that the NH_2-terminal ~40 amino acid amphipathic regions of endophilin I and B1 are required for in vitro lipid binding and liposome tubulation activity of these proteins (Farsad et al., 2001). Furthermore, it has been also demonstrated that enzymatic LPA acyl transferase activity, located within the NH_2-terminal region, is potentially important for the function of these proteins (Schmidt et al., 1999). We tested whether or not expression of a YFP-tagged NH_2-terminal 59 amino acid membrane active domain of endophilin B1 (endoB$^{1\text{-}59\Delta C}$-YFP) or a protein lacking this domain (endoB$^{60\text{-}362\Delta N}$-YFP) would affect the mitochondrial morphology, as well as OMM and IMM compartment synchrony. Confocal microscopy analyses of cells stained with Mitotracker showed distinct alterations in the shape of mitochondria in cells expressing endoB$^{60\text{-}362\Delta N}$-YFP (Fig. 5, A and C), but not the three other constructs tested, endoB$^{1\text{-}59\Delta C}$-YFP (Fig. 5, B and C), YFP-tagged endophilin B1 (endoB-YFP), and YFP vector (not depicted). Mitochondrial defects observed in endoB$^{60\text{-}362\Delta N}$-YFP–expressing cells resemble those in endoB RNAi cells and include marked redistribution of these organelles to the perinuclear area and an increase in the mitochondrial diameter variability. However, formation of interconnected, ring-shaped mitochondria, (type I and II; Fig. 1 Dc) is less pronounced compared with endoB RNAi cells. In cells expressing endoB$^{60\text{-}362\Delta N}$-YFP, a dissociation of OMM compartment from the matrix was also detected (Fig. 5 D). Altogether, these data indicate expression of endoB$^{60\text{-}362\Delta N}$-YFP induces dominant-negative inhibition of endogenous endophilin B1, confirming the RNAi data implicating endophilin B1 in the maintenance of mitochondrial network distribution and morphology.

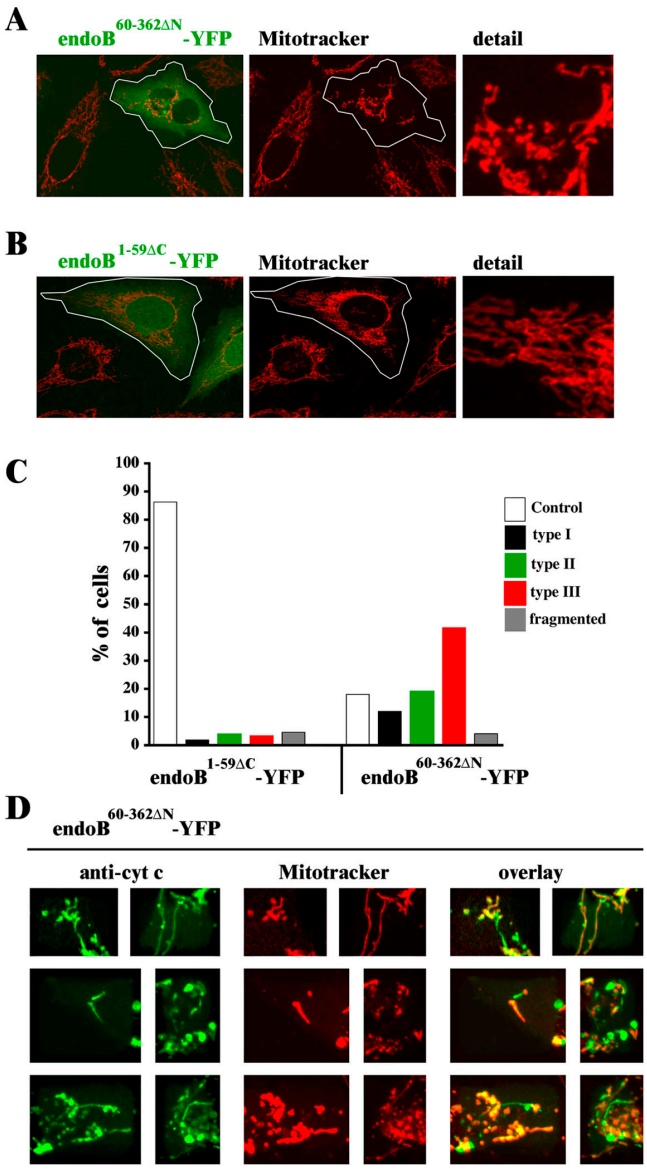

Figure 5. **Overexpression of NH_2-terminal truncated endophilin B1 induces mitochondrial morphology defects.** HeLa cells were transfected with endoB$^{60\text{-}362\Delta N}$-YFP (A) and with endoB$^{1\text{-}59\Delta C}$-YFP (B) and analyzed by confocal microscopy. (C) Mitochondrial phenotypes were scored within endoB$^{60\text{-}362\Delta N}$-YFP– and endoB$^{1\text{-}59\Delta C}$-YFP–expressing cells (n = 400). (D) OMM/IMM synchrony was assayed in endoB$^{60\text{-}362\Delta N}$-YFP–expressing cells. Cells were labeled with Mitotracker (red), stained with anti–cytochrome *c* mAbs (green), and analyzed by confocal microscopy. Note apparent dissociation of OMM compartment from matrix.

Dynamic association of endophilin B1 with mitochondria

If endophilin B1 is directly required for the maintenance of mitochondrial dynamics, then it may localize to these organelles. We examined the subcellular distribution of endophilin B1 in living HeLa cells expressing endoB-YFP (Fig. 6 A) and in fixed cells by immunostaining endogenous protein with anti–endophilin B1 mAbs (Fig. 6 B and Fig. 1 Ba). We found that although a small subpopulation of this protein can be detected colocalizing with mitochondria (Fig. 6 B), most endophilin B1 appears to reside in the cytosol. Results similar to those in HeLa cells were obtained when endoB-YFP–expressing or anti–endophilin B1 mAbs stained, Cos7 cells were examined (unpublished data). This subcellular localization of endophilin B1 was further confirmed by cell fractionation that revealed that, as in the case of cytosolic proteins known to have an ability to dynamically interact with OMM, such as Drp1 and Bax (Wolter et al., 1997; Labrousse et al., 1999), only a minor part of the endophilin B1 cofractionated with the mitochondria-enriched heavy membrane fraction, and a majority appears as a soluble cytosolic protein (Fig. 6 C). We postulated that, like several membrane modifying proteins, including endophilin I in the synapse (Schmidt and Huttner, 1998) and Drp1 during scission

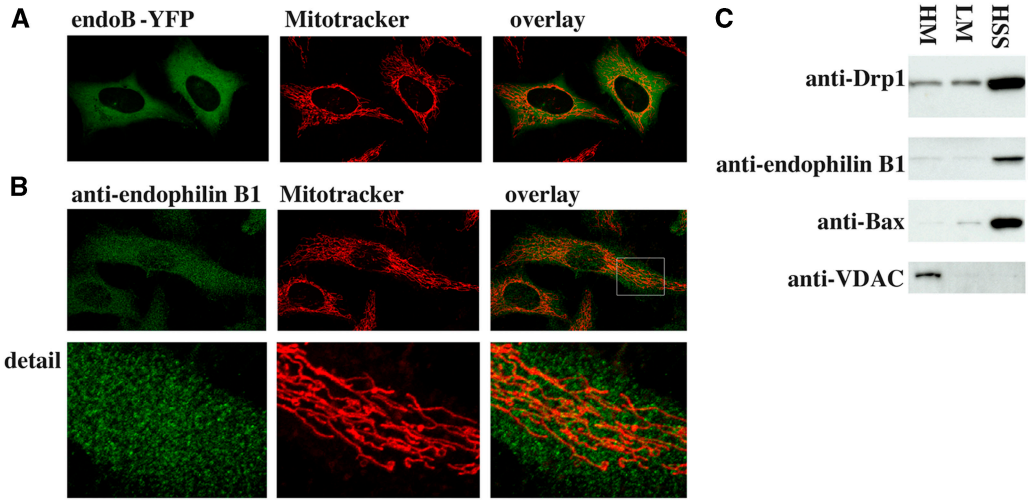

Figure 6 (continues on facing page)

of mitochondria (Labrousse et al., 1999; Smirnova et al., 2001), endophilin B1 may cycle between the cytosol and the target membranes and, at any one time, only a small pool of active protein may reside at the OMM. It has been shown that during apoptosis mitochondria transform from an elongated, interconnected network into fragmented, round organelles. Unlike asynchronous division of mitochondria in interphase cells, apoptotic fragmentation of these organelles occurs synchronously within several minutes (Frank et al., 2001; Karbowski and Youle, 2003). Because proteins involved in the regulation of mitochondrial morphology, including Drp1, Fis1, and Opa1 (Frank et al., 2001; Olichon et al., 2002; James et al., 2003), participate in apoptotic remodeling of these organelles, we examined whether or not endophilin B1 is activated during apoptosis. Cos7 cells were transfected with endoB-YFP, and, to accelerate apoptosis, with a proapoptotic protein from the Bcl-2 family, Bax. Cells were treated with the apoptosis inducer STS, followed by time-lapse confocal analyses of the subcellular distribution of endoB-YFP. A gradual redistribution of endoB-YFP into concentrated clusters, starting an hour or two after the addition of STS (Fig. 6 Dc, ~90 min in the example shown) that increase in number within minutes after initiation (Fig. 6 D, c–e), and before terminal decomposition of apoptotic cells (Fig. 6 Df) was detected. To test if the focal patches of endoB-YFP are associated with mitochondria, cells were cotransfected with endoB-YFP (Fig. 6, E and F, green), pcDNA3.1-Bax (Fig. 6 E), and transfected with mito-DsRED2 (Fig. 6 E) or labeled with Mitotracker (Fig. 6 F) to reveal mitochondria followed by pretreatment with the broad specificity caspase inhibitor 75 μM zVAD-fmk and treatment with 1 μM STS for 90 min (Fig. 6 E) or another inducer of apoptosis, ActD, for 36 h (Fig. 6 F). Colocalization of endoB-YFP with mitochondrial markers could be detected in all cells with punctate endoB-YFP fluorescence patterns. In some cases, endoB-YFP clusters localized on the tips or along mitochondrial tubules, and in others in ring-like patterns encircling round mitochondria were detected (Fig. 6, E and F; more examples of the submitochondrial localization of endoB-YFP are shown in Fig. S1, available at http://www.jcb.org/cgi/content/full/jcb.200407046/DC1). Interestingly, not all mitochondria within a single cell were associated with detectable levels of endoB-YFP (Fig. 6, E and F, arrows), and the number of endophilin B1 patches varied within different cells (not depicted). Moreover, unlike mitochondrial accumulation of Bax that can be detected in increasing numbers of cells upon apoptosis (Wolter et al., 1997), the total number of cells with mitochondria-associated endophilin B1 does not increase after the initial detection, suggesting that mitochondrial accumulation of endophilin B1 is transient (unpublished data). We also found that in Cos7 cells treated with ActD, endogenous endophilin B1 redistributes to mitochondria (Fig. 6 G) in a similar manner as endoB-YFP.

Altogether, our data shows increased association of endophilin B1 with mitochondria during apoptosis, indicating a transient, regulated nature of endophilin B1 interaction with these organelles. We speculate that endophilin B1 also cycles between cytosol and mitochondria in healthy cells.

Drp1 is required for the formation of the endoB RNAi mitochondrial phenotype

The results described in this work, together with published data (Labrousse et al., 1999; Smirnova et al., 2001), suggest that partial conservation of an endocytosis-like membrane shaping mechanism(s) participates in the regulation of the OMM dynamics, with Drp1 playing the role of dynamin and endophilin B1 taking the part of endophilin I. To test if Drp1 is required for the formation of the mitochondrial phenotype detected in endoB RNAi cells, we examined the mitochondrial morphology in cells depleted of both proteins (endoB/Drp1 RNAi cells). HeLa cells transfected with endoB RNAi or Drp1 RNAi constructs or cotransfected with both constructs followed by selection with hygromycin were analyzed for levels of endophilin B1 and Drp1 (Fig. 7 A) and mitochondrial morphology (Fig. 7, B and C). Western blot analyses revealed a degree of down-regulation of both proteins in the endoB/Drp1 double RNAi cells only slightly less pronounced than observed in each single knockdown (Figs. 7 A, 1 A, and 4 E). EndoB RNAi, Drp1 RNAi, and endoB/Drp1 RNAi cells stained with Mitotracker were analyzed by confocal microscopy (Fig. 7 B). We found that depletion of

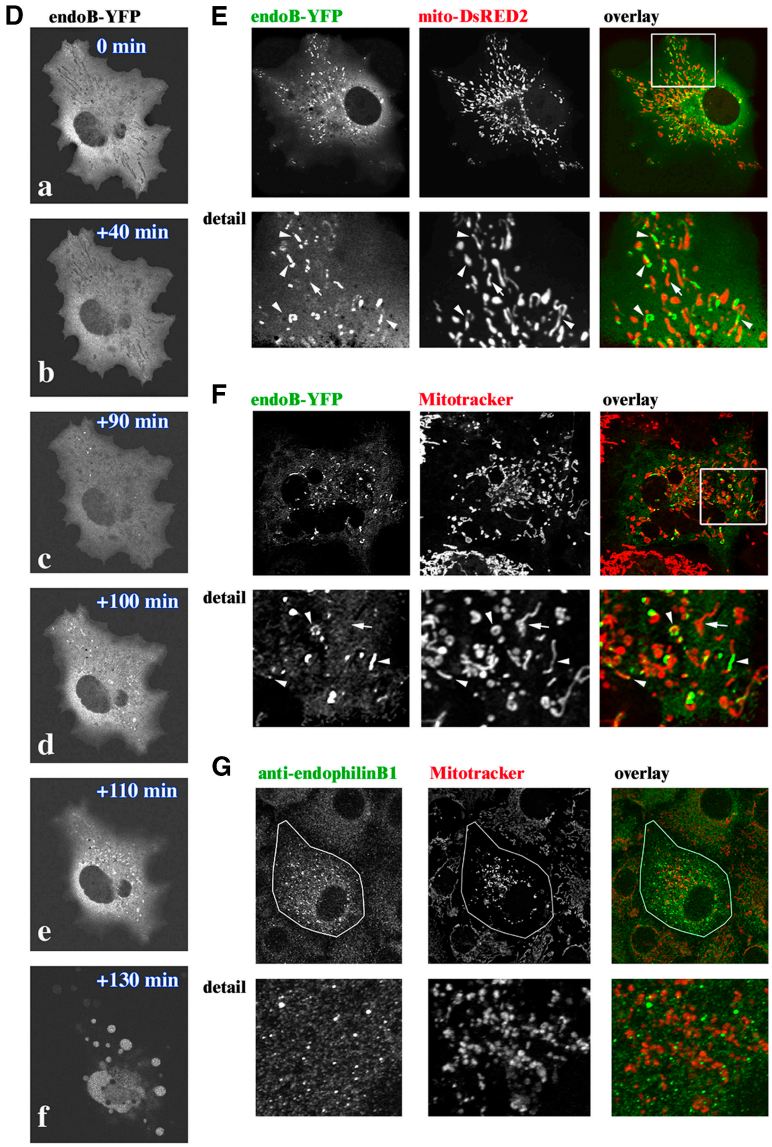

Figure 6. **Dynamic association of endophilin B1 with mitochondria.** HeLa cells were transfected with endoB-YFP (A, green) or stained with anti–endophilin B1 mAbs (B, green), labeled with Mitotracker to reveal mitochondria (A and B, red), and analyzed by confocal microscopy. (C) Cells were fractionated using differential centrifugation to obtain a mitochondria-enriched heavy membrane fraction (HM), a light membrane fraction (LM), and a high speed supernatant-containing soluble cytosolic proteins (HSS), and subjected to SDS PAGE and Western blot analysis to reveal the subcellular distribution of endophilin B1. Anti-Bax mAbs were used as a marker of the cytosol and anti-VDAC mAbs for mitochondria. (D) Cos7 cells transfected with pcDNA3-Bax and endoB-YFP were treated with 1 μM STS and analyzed by time-lapse confocal microscopy for the subcellular distribution of endophilin B1. Note the clustering of endoB-YFP detectable before apoptotic decomposition of the cells (c–e). To analyze the spatial relation of endoB-YFP patches and mitochondria, cells were transfected with endoB-YFP (E and F, green) or stained with anti–endophilin B1 mAbs (G, green) to reveal the subcellular distribution of endophilin B1 and labeled with Mitotracker (F and G, red) or transfected with mito-DsRED2 (E, red) to reveal mitochondria, followed by treatment with the caspase inhibitor zVAD-fmk and STS for 90 min (E) or with zVAD-fmk and ActD for 36 h (F, and G), and examined by confocal microscopy. Note the mitochondrial localization of endoB-YFP patches.

Drp1 together with endophilin B1 resulted in the formation of highly interconnected networks of mitochondria, indistinguishable from that observed in Drp1 RNAi cells (Figs. 7 B and 4 F). Only ∼9% of endoB/Drp1 RNAi cells had a mitochondrial phenotype resembling type I–III endoB RNAi phenotypes and in ∼90% of the endoB/Drp1 RNAi cells mitochondria formed highly interconnected structures characteristic for single Drp1 RNAi (Fig. 7 C). Moreover, the separation of the OMM and the IMM compartments is no longer detectable (Fig. 7 D). We also analyzed the mitochondrial morphology (Fig. 7 E) and OMM/IMM synchrony (not depicted) in endoB RNAi cells transfected with a dominant-negative mutant of Drp1 ($Drp1^{K38A}$). Overexpression of $Drp1^{K38A}$ has been reported to result in the formation of elongated, interconnected mitochondria, which is consistent with an inhibition of endogenous protein (Labrousse et al., 1999; Smirnova et al., 2001). We detected, in ∼100% of the endoB RNAi cells expressing $Drp1^{K38A}$ (Fig. 7 E, arrows), a mitochondrial phenotype and OMM/IMM synchrony (not depicted) characteristic for $Drp1^{K38A}$ expression alone. These data confirm the results obtained with endoB/Drp1 RNAi cells and further suggest that an activity of Drp1 is required for formation of the endoB RNAi mitochondrial phenotype.

We conclude that Drp1 may act upstream of endophilin B1 in the regulation of mitochondrial membrane dynamics and mediate or regulate the formation of the vesicular and tubular structures containing OMM but not IMM compartments. Participation of an intermediate mediator cannot be excluded. Interestingly, it has been shown that overexpression of a "mitochondrial" isoform of synaptojanin, synaptojanin 2A, a homologue of the protein coparticipating with the dynamin and endophilin I in endocytotic vesicle formation, results in distinct changes to the mitochondrial network morphology (Nemoto and De Camilli, 1999).

Discussion

In this work, we demonstrate a role of endophilin B1 in the maintenance of mitochondrial morphology in mammalian cells. In cells depleted of endophilin B1 by shRNAi and analyzed by confocal microscopy, the distribution and shape of

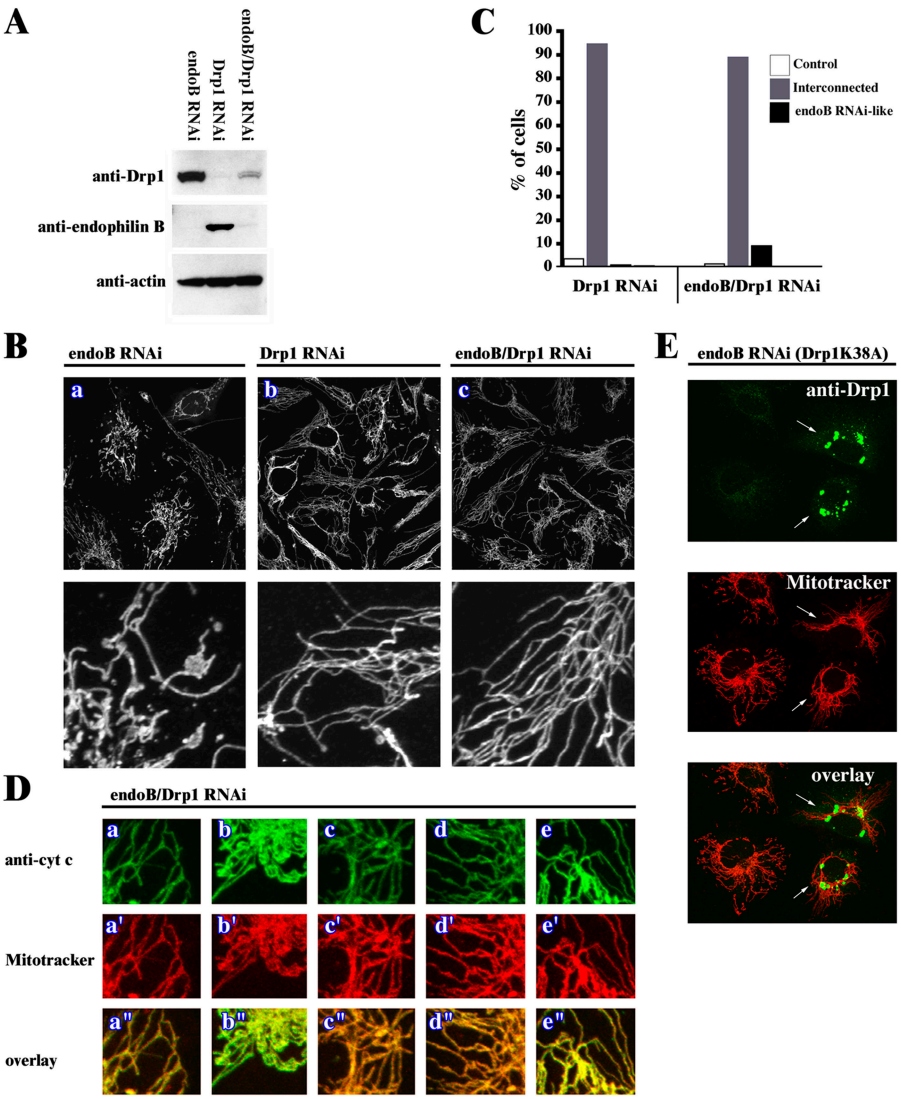

Figure 7. **Phenotypic consequences of simultaneous down-regulation of endophilin B1 and Drp1.** HeLa cells were transfected with endoB RNAi and Drp1 RNAi constructs separately or combined. Cells were selected with hygromycin for 4 d and analyzed for protein levels by Western blot (A) and, after staining with Mitotracker (B and D, a′–e′) and anti–cytochrome *c* mAbs (D, a–e), analyzed by confocal microscopy. (C) Phenotypes of mitochondria in Drp1 RNAi and endoB/Drp1 RNAi cells were scored ($n = 400$). (E) EndoB RNAi cells were transfected with a DN mutant of Drp1, $Drp1^{K38A}$ (arrows), labeled with Mitotracker (red), stained with anti-Drp1 mAbs (green), and analyzed by confocal microscopy. Complete reversal of the endophilin B1 single RNAi phenotype and formation of Drp1-like single RNAi phenotype cells in endoB/Drp1 double RNAi cells indicates that Drp1 may be an upstream factor of endophilin B1 in the chain of events leading to mitochondrial division.

the mitochondria were altered, whereas the morphology of several other organelles appeared normal. Moreover, a simultaneous imaging of OMM and mitochondrial matrix in endoB RNAi cells revealed an apparent physical dissociation of these compartments and the formation of vesicular and tubular OMM structures. To our knowledge, this is the first description of asynchronous behavior of OMM and IMM compartments in mammalian cells. We also found that endophilin B1 is a cytosolic protein, partially colocalizing and cofractionating with mitochondria. In normally growing cells only a small fraction of endophilin B1 localizes to mitochondria. However, upon activation of apoptosis, a process associated with massive, simultaneous remodeling of these organelles, endophilin B1 was found to accumulate into concentrated patches that colocalized with mitochondria. Altogether our data indicate that endophilin B1 is a component of the molecular machinery participating in the modeling of the OMM. Endophilin B1 may cycle on and off mitochondria, and transient interactions of this protein with the OMM may be essential for maintenance of their morphology.

Reversible localization of proteins to membranes, such as GTPase-regulated membrane interaction of certain Rab proteins, or cyclic assembly and disassembly of SNAREs (Chen et al., 1999; Jahn, 2004), are essential for their functions during membrane fusion. Mitochondrial dynamics are also regulated by transient interactions of cytosolic proteins with the OMM. For example, Drp1 normally resides in the cytosol and only a small fraction of this protein is associated with mitochondria, peroxisomes, and other membrane structures (Yoon et al., 1998; Smirnova et al., 2001; Koch et al., 2003). However, treatment with the phorbol ester, PMA (Labrousse et al., 1999), elevation of subcellular Ca^{2+} (Breckenridge et al., 2003), and induction of apoptosis (Frank et al., 2001) all lead to mitochondrial accumulation of this GTPase, formation of punctate "scission foci," followed by GTP hydrolysis-dependent mitochondrial division and disassembly of multimeric Drp1 complexes, indicative of a regulated, dynamic nature of Drp1 OMM interactions.

We propose that transient interactions of endophilin B1 with mitochondria are required for remodeling of the OMM. Members of the endophilin protein family, and a group of proteins sharing an NH_2-terminal BAR domain with endophilins, participate at several subcellular locations

in the regulation of membrane curvature, a process required for membrane scission (Schmidt et al., 1999; Weigert et al., 1999; Habermann, 2004). For example, BARS-50, a protein with intrinsic LPA acyltransferase activity, is required for scission of Golgi tubules into vesicular structures. As in the case of endophilins, the activity of BARS-50 depends on the enzymatic conversion of LPA into PA. Moreover, it has been also shown that this conversion is sufficient to cause Golgi tubule scission (Weigert et al., 1999), suggesting a common mechanism of membrane scission involving the remodeling of membrane lipids. Consistent with a potential role of the membrane modifying activity of endophilin B1 in the regulation of mitochondrial dynamics is the spatial dissociation of the OMM and the IMM induced by the overexpression of a truncated variant of this protein lacking its lipid transferase NH_2-terminal domain. Interestingly, inhibition of endophilin I resulted in an accumulation of invaginated plasma membrane intermediates (Gad et al., 2000), somewhat resembling the vesicular and tubular OMM structures shown here, suggesting that a similar cascade of events may regulate plasma membrane remodeling and certain aspects of OMM dynamics. However, currently we cannot clarify whether the OMM structures induced by endophilin B1 inactivation are intermediates of an as yet unrecognized OMM trafficking pathway, analogous to the vesicle intermediates in endocytosis, or whether they result from the inhibition of a known mitochondrial process. Studies of ERP1, a *C. elegans* homologue of endophilin B1, as well as some of the data shown here, suggest that endophilin B1 participates in mitochondrial division. Overexpression of ERP1 can regulate mitochondrial connectivity and cause fragmentation of these organelles. Moreover, ERP1 was found to colocalize with Drp1-enriched mitochondrial fission foci leading to the conclusion that ERP1 may be involved in mitochondrial division in *C. elegans* (van der Bliek, A., personal communication). One feature consistent with ERP1 participating in mitochondrial fission in *C. elegans*, the formation of mitochondria with unusual branching patterns, was also detected in HeLa cells deficient in endophilin B1 (Video 1). However, depletion of Drp1 in HeLa cells causes a more distinct increase in mitochondrial connectivity than that detected in endoB RNAi cells, indicating that endophilin B1 may have a more marginal and less rate-limiting role in mitochondrial division in mammalian cells than in *C. elegans* and might act as one of the downstream factors regulating OMM coordination with IMM remodeling. Higher variability of mitochondrial phenotypes in endoB RNAi, as compared with Drp1 RNAi cells as well as an apparent gradation of the extent to which OMM vesicular and tubular structures are formed in endoB RNAi cells further suggests roles of additional factors in the process of endophilin B1 regulation of mitochondrial morphology. We speculate that in this scenario endophilin B1 would act late in the sequence of mitochondrial scission events that normally couple OMM morphology to the IMM morphology. A defect in OMM scission subsequent to IMM scission would lead to the phenotypes detected in endoB RNAi cells, aberrantly shaped mitochondria, as well as abnormal separation of the two mitochondrial membranes. We also found that inactivation of Drp1, either by performing double knockdown of endophilin B1 and Drp1 or overexpression of a DN mutant of Drp1, $Drp1^{K38A}$, in endoB RNAi cells, leads to a complete suppression of the endoB RNAi phenotype, which is consistent with Drp1 acting upstream of endophilin B1 in the maintenance of mitochondrial network dynamics. An existence of factors essential for coordinate scission of both membranes, in addition to more specialized proteins required for completion of the scission of either of the two mitochondrial membranes, is supported by reports describing morphological consequences of mutations of proteins required for mitochondrial division in *Saccharomyces cerevisiae* (Osteryoung and Nunnari, 2003). Single inactivation of Dnm1, Fis1, or Mdv1 resulted in similar planar net-like morphologies of mitochondria, signifying essential roles of each of these proteins for the scission of both OMM and IMM (Osteryoung and Nunnari, 2003). However, sheets, rings, and mitochondrial spheres were found upon mutation in Mdm33 (Messerschmitt et al., 2003), an integral protein of the IMM that are distinct from the planar net-like mitochondria detectable in Dnm1/Mdv1/Fis1 mutants. Furthermore, when overexpressed, Mdm33 induces several defects of the IMM, including septation and formation of detached vesicular structures, which is consistent with a specific role of this protein in maintenance of the structure of IMM. Thus, it has been proposed that Mdm33 participates in the regulation of IMM scission (Messerschmitt et al., 2003). Moreover, it has been also shown that the Δmdm33 defects are epistatic to the Δfis1 mitochondrial morphology (Messerschmitt et al., 2003), indicating independent functions of these proteins in mitochondrial division. We propose that, in addition to the core complex (Dnm1-, Mdv1-, and Fis1-like proteins) that may be responsible for a coordinate initiation as well as some aspects of progression of both mitochondrial membranes scission, additional IMM- and OMM-specific factors (Mdm33- and endophilin B1–like proteins, respectively) are required for completion of the scission of mitochondria. SH3GLB2, another endophilin-like protein that has been found to interact with endophilin B1(Pierrat et al., 2001), is an additional candidate for a protein that may participate in the OMM remodeling. Analyses of the consequences of down-regulation of SH3GLB2 alone or combined with endophilin B1 will help establish a more comprehensive picture of the role of endophilin-like proteins in the maintenance of mitochondrial membrane dynamics.

In summary, we describe the role of the fatty acyl transferase, endophilin B1, in the regulation of mitochondrial morphology and OMM dynamics, extending the general understanding of the processes governing mitochondrial dynamics. Further experiments, aiming at identification of how these proteins work together in IMM and OMM remodeling, will allow insight into the complex, multilevel process of mitochondrial membrane homeostasis regulation.

Materials and methods

Cell culture and transfection

HeLa and Cos7 cells were grown as described previously (Karbowski et al., 2004) and were transfected with FuGENE (Roche) according to the manufacturer's instructions.

Cloning, RNAi, and mutagenesis

The human endophilin B1 cDNA was cloned from fetal human brain mRNA (Stratagene) by RT-PCR. A first-strand cDNA was synthesized from

the mRNA by SuperScript II reverse transcriptase (Invitrogen) with 0.5 μg of oligo(dT) primer and random primer according to manufacturer's instructions. The PCR amplification for endophilin B1 cDNA was performed using the first-strand cDNA as a template with *Pfu turbo* polymerase (Stratagene). The sequences of oligonucleotide primers used for PCR were 5′-GTCAGATCTGCCATGAATATCATGGACTTCAACGTGAAG-3′ and 5′-ACTGAATT**C**CATAGTCCACCTACTTAATTGAGCAG-3′. The PCR product was cloned into BamHI and EcoRI sites of pcDNA 3.1 plasmid vector (Invitrogen).

Episomal pREP4 (Invitrogen)-based vectors containing RNA-silencing shRNA (Paddison et al., 2002) downstream of a U6 promoter were used for RNAi. Two complementary DNA oligonucleotides bearing target sequence, Hind III linker, and U6 terminator were synthesized, annealed, and ligated into BseRI and BamHI sites of pSHAG-1 vector. For long-term suppression of gene expression by shRNA, the region encoding U6 promoter and shRNA in pSHAG-1 was subcloned into NotI and BamHI sites of pREP4. Target sequences used were as follows: 5′-atcattgttgttagtctgaagacactgtc-3′ for endophilin B1 (GenBank/EMBL/DDBJ accession no. NM 016009.2) and 5′-ttcaatccgtgatgagtatgcttttcttc-3′ for Drp1 (GenBank/EMBL/DDBJ accession no. NM 012062). The target sequence for the control shRNA against GFP was 5′-GAAGTTCGAGGGCGACACCCTGGTGAACC-3′. For reconstitution of endophilin B1 expression in endoB RNAi cells five silent nucleotide mutations were engineered within endophilin B1 sequence targeted by RNAi using QuikChange Site-Directed Mutagenesis Kit (Stratagene) with the following primers: 5′-CAATTATCTTAGTAACAACAATCAAACAGCGTGACACCTGTACCATCAG-3′ and 5′-CTGATGGTACAGGTGTCACGCTCGTTTGATTGTTGTTACTAAGATAATTG-3′.

The following primers introducing EcoRI at the NH_2 terminus and BamHI at the COOH terminus were used to construct YFP-tagged variants of endophilin B1: (A) 5′-CGGTAGCGTGAATTCGTGAATGAATATCATGGACTTCAACGTG-3′; (B) 5′-CGCCATTGCTGGATCCGGATTGAGCAGTTCTAAGTAGGT-3′; (C) 5′-CGGTAGCGTGAATTCGTGATGAAACAAACTGAAGTG-3′; and (D) 5′-CGCCATTGCTGGATCCGGTATTTTTTCTGTCCATAT-3′. Primers A and B were used to obtain wild-type and endoB-YFP, primers A and D for endo$B^{1\text{-}59\Delta C}$-YFP, and primers C and B for endo$B^{60\text{-}362\Delta N}$-YFP. PCR products were digested with EcoRI and BamHI and cloned into YFP-N1 expression vector (CLONTECH Laboratories, Inc.). Peroxisomes were visualized using a peroxisome-targeting sequence fused to CFP (peroxi-CFP; CLONTECH Laboratories, Inc.). Mitochondrial matrix was visualized using mito-YFP (CLONTECH Laboratories, Inc.) or mito-DsRED2 (Karbowski et al., 2002) constructs. Mito-PAGFP, a photoactivatable marker of the mitochondrial matrix, and YFP- Fis1 constructs were described previously (Karbowski et al., 2002, 2004).

Antibodies and immunostaining

The following primary antibodies were used in this study: anti–cytochrome *c* mAbs (clone 6H2.B4; BD Biosciences), anti-AIF pAbs (clone H-300; Santa Cruz Biotechnology, Inc.), anti-Drp1 mAbs (clone 8; Transduction Laboratories), anti-Bif1 (endophilin B1) mAbs (clone 30A882; Imgenex), anti-actin mAbs (clone AC-40; Sigma-Aldrich), anti-EEA1 (clone 14; Transduction Laboratories), anti-BiP/GRP78 mAbs (clone 40; Transduction Laboratories), anti-Rab11 mAbs (clone 47; Transduction Laboratories), anti-GM130 mAbs (clone 35; Transduction Laboratories), anti-Bax mAbs (1F6; Hsu and Youle, 1997), and anti-mitochondrial porin (VDAC) mAbs (clone 20B12; Molecular Probes). For immunofluorescence microscopy, cells grown in 2-well chamber slides (model 1 German borosilicate; Labtec) were fixed for 30 min with 4% PFA in PBS, stained with primary antibodies, followed by staining with goat anti–mouse, goat anti–rabbit Alexa Fluor 488 antibodies (Molecular Probes), or goat anti–mouse Alexa Fluor 633 antibodies (Molecular Probes). For detection of lysosomes, cells were stained with 50 nM of Lysotracker red DND-99 (Molecular Probes). To visualize the mitochondrial matrix, 50 nM of Mitotracker red CMXRos (Molecular Probes) was added to the cells 30 min before fixation.

Subcellular fractionation and immunoblotting

For subcellular fractionation, cells were collected washed in PBS, resuspended in the lysis buffer (10 mM Hepes/KOH, pH 7.4, 38 mM NaCl supplemented with 1 mM PMSF, 10 μg/ml leupeptin, and 2 μg/ml aprotinin), and incubated on ice for 45 min. Cells were broken using a Dounce homogenizer followed by a series of centrifugations: 500 *g* for 5 min, yielding a pellet (P1) consisting of nuclei and unbroken cells and a supernatant that was further centrifuged at 6,000 *g* for 15 min, yielding P2 (heavy membrane fraction) and a supernatant that was centrifuged at 250,000 *g*, yielding P3 (light membrane fraction) and a supernatant that was used as a cytosolic fraction (C).

For total cell extracts, cells were collected, washed with PBS, and resuspended in SDS PAGE sample buffer, incubated at 99°C for 10 min. An aliquot of the sample was used to determine protein concentration. Protein was separated on 4–20% gradient polyacrylamide gels (Invitrogen), transferred onto PVDF membranes (Immubilon-P; Millipore), and incubated with primary antibodies, followed by HRP-conjugated anti–mouse secondary antibody. Blots were detected with ECL PLUS (Amersham Biosciences).

Confocal microscopy and image analysis

Images were captured with a microscope (model LSM 510; Carl Zeiss MicroImaging, Inc.) using a 63 × 1.4 NA Apochrome objective (Carl Zeiss MicroImaging, Inc.). The excitation wavelengths were 488 nm for Alexa Fluor 488 antibodies or mito-PAGFP, 543 nm for Mitotracker, and 630 nm for Alexa Fluor 633 antibodies. Projected series of z-sections collected with intervals of 0.5–0.75 μm between sections are shown.

413-nm light was used for photoactivation of mito-PAGFP, as described previously (Karbowski et al., 2004). Regions of interest were selected and a series of z-sections from the top of the cell to the bottom with intervals set to 0.5–0.75 μm were irradiated with 413-nm light. The same intervals were used for imaging. Postacquisition processing was performed with MetaMorph and Microsoft Excel software for photoactivation experiments and with image viewer (model LSM510; Carl Zeiss MicroImaging, Inc.) for measurements of the mitochondrial diameter.

Online supplemental material

Video 1 shows mitochondrial plasticity in endoB RNAi cells. Fig. S1 shows submitochondrial localization of endoB-YFP in apoptotic Cos7 cells. Online supplemental material is available at http://www.jcb.org/cgi/content/full/jcb.200407046/DC1.

The authors thank J. Barrick and M. Brown for technical assistance and C.L. Smith (National Institute of Neurological Disorders and Stroke, Leigh Imaging Facility) for assistance with confocal microscopy.

This work was supported by the National Institute of Neurological Disorders and Stroke, National Institutes of Health.

Submitted: 9 July 2004
Accepted: 12 August 2004

References

Breckenridge, D.G., M. Stojanovic, R.C. Marcellus, and G.C. Shore. 2003. Caspase cleavage product of BAP31 induces mitochondrial fission through endoplasmic reticulum calcium signals, enhancing cytochrome c release to the cytosol. *J. Cell Biol.* 160:1115–1127.

Chen, Y.A., S.J. Scales, S.M. Patel, Y.C. Doung, and R.H. Scheller. 1999. SNARE complex formation is triggered by Ca^{2+} and drives membrane fusion. *Cell.* 97:165–174.

Cuddeback, S.M., H. Yamaguchi, K. Komatsu, T. Miyashita, M. Yamada, C. Wu, S. Singh, and H.-G. Wang. 2001. Molecular cloning and characterization of Bif-1. A novel Src homology 3 domain-containing protein that associates with Bax. *J. Biol. Chem.* 276:20559–20565.

Degli Esposti, M., and C. Dive. 2003. Mitochondrial membrane permeabilisation by Bax/Bak. *Biochem. Biophys. Res. Commun.* 304:455–461.

Dimmer, K.S., S. Fritz, F. Fuchs, M. Messerschmitt, N. Weinbach, W. Neupert, and B. Westermann. 2002. Genetic basis of mitochondrial function and morphology in *Saccharomyces cerevisiae*. *Mol. Biol. Cell.* 13:847–853.

Farsad, K., N. Ringstad, K. Takei, S.R. Floyd, K. Rose, and P. De Camilli. 2001. Generation of high curvature membranes mediated by direct endophilin bilayer interactions. *J. Cell Biol.* 155:193–200.

Frank, S., B. Gaume, E.S. Bergmann-Leitner, W.W. Leitner, E.G. Robert, F. Catez, C.L. Smith, and R.J. Youle. 2001. The role of dynamin-related protein 1, a mediator of mitochondrial fission, in apoptosis. *Dev. Cell.* 1:515–525.

Frieden, M., D. James, C. Castelbou, A. Danckaert, J.C. Martinou, and N. Demaurex. 2004. Ca^{2+} homeostasis during mitochondrial fragmentation and perinuclear clustering induced by hFis1. *J. Biol. Chem.* 279:22704–22714.

Gad, H., N. Ringstad, P. Low, O. Kjaerulff, J. Gustafsson, M. Wenk, G. Di Paolo, Y. Nemoto, J. Crun, M.H. Ellisman, et al. 2000. Fission and uncoating of synaptic clathrin-coated vesicles are perturbed by disruption of interactions with the SH3 domain of endophilin. *Neuron.* 27:301–312.

Habermann, B. 2004. The BAR-domain family of proteins: a case of bending and binding? *EMBO Rep.* 5:250–255.

Hales, K.G., and M.T. Fuller. 1997. Developmentally regulated mitochondrial fu-

sion mediated by a conserved, novel, predicted GTPase. *Cell.* 90:121–129.

Herlan, M., C. Bornhovd, K. Hell, W. Neupert, and A.S. Reichert. 2004. Alternative topogenesis of Mgm1 and mitochondrial morphology depend on ATP and a functional import motor. *J. Cell Biol.* 165:167–173.

Hinshaw, J.E. 2000. Dynamin and its role in membrane fission. *Annu. Rev. Cell Dev. Biol.* 16:483–519.

Hsu, Y.T., and R.J. Youle. 1997. Nonionic detergents induce dimerization among members of the Bcl-2 family. *J. Biol. Chem.* 272:13829–13834.

Huttner, W.B., and A. Schmidt. 2000. Lipids, lipid modification and lipid-protein interaction in membrane budding and fission–insights from the roles of endophilin A1 and synaptophysin in synaptic vesicle endocytosis. *Curr. Opin. Neurobiol.* 10:543–551.

Jahn, R. 2004. Principles of exocytosis and membrane fusion. *Ann. NY Acad. Sci.* 1014:170–178.

James, D.I., P.A. Parone, Y. Mattenberger, and J.C. Martinou. 2003. hFis1, a novel component of the mammalian mitochondrial fission machinery. *J. Biol. Chem.* 278:36373–36379.

Karbowski, M., and R.J. Youle. 2003. Dynamics of mitochondrial morphology in healthy cells and during apoptosis. *Cell Death Differ.* 10:870–880.

Karbowski, M., Y.-J. Lee, B. Gaume, S.-Y. Jeong, S. Frank, A. Nechushtan, A. Santel, M. Fuller, C.L. Smith, and R.J. Youle. 2002. Spatial and temporal association of Bax with mitochondrial fission sites, Drp1, and Mfn2 during apoptosis. *J. Cell Biol.* 159:931–938.

Karbowski, M., D. Arnoult, H. Chen, D.C. Chan, C.L. Smith, and R.J. Youle. 2004. Quantitation of mitochondrial dynamics by photolabeling of individual organelles shows that mitochondrial fusion is blocked during the Bax activation phase of apoptosis. *J. Cell Biol.* 164:493–499.

Koch, A., M. Thiemann, M. Grabenbauer, Y. Yoon, M.A. McNiven, and M. Schrader. 2003. Dynamin-like protein 1 is involved in peroxisomal fission. *J. Biol. Chem.* 278:8597–8605.

Labrousse, A.M., M.D. Zappaterra, D.A. Rube, and A.M. van der Bliek. 1999. *C. elegans* dynamin-related protein DRP-1 controls severing of the mitochondrial outer membrane. *Mol. Cell.* 4:815–826.

Legros, F., A. Lombes, P. Frachon, and M. Rojo. 2002. Mitochondrial fusion in human cells is efficient, requires the inner membrane potential, and is mediated by mitofusins. *Mol. Biol. Cell.* 13:4343–4354.

Messerschmitt, M., S. Jakobs, F. Vogel, S. Fritz, K.S. Dimmer, W. Neupert, and B. Westermann. 2003. The inner membrane protein Mdm33 controls mitochondrial morphology in yeast. *J. Cell Biol.* 160:553–564.

Mozdy, A.D., and J.M. Shaw. 2003. A fuzzy mitochondrial fusion apparatus comes into focus. *Nat. Rev. Mol. Cell Biol.* 4:468–478.

Nakada, K., K. Inoue, T. Ono, K. Isobe, A. Ogura, Y.I. Goto, I. Nonaka, and J.I. Hayashi. 2001. Inter-mitochondrial complementation: Mitochondria-specific system preventing mice from expression of disease phenotypes by mutant mtDNA. *Nat. Med.* 7:934–940.

Nangaku, M., R. Sato-Yoshitake, Y. Okada, Y. Noda, R. Takemura, H. Yamazaki, and N. Hirokawa. 1994. KIF1B, a novel microtubule plus end-directed monomeric motor protein for transport of mitochondria. *Cell.* 79:1209–1220.

Nemoto, Y., and P. De Camilli. 1999. Recruitment of an alternatively spliced form of synaptojanin 2 to mitochondria by the interaction with the PDZ domain of a mitochondrial outer membrane protein. *EMBO J.* 18:2991–3006.

Olichon, A., L. Baricault, N. Gas, E. Guillou, A. Valette, P. Belenguer, and G. Lenaers. 2002. Loss of OPA1 perturbates the mitochondrial inner membrane structure and integrity, leading to cytochrome c release and apoptosis. *J Biol. Chem.* 278:7743–7746.

Osteryoung, K.W., and J. Nunnari. 2003. The division of endosymbiotic organelles. *Science.* 302:1698–1704.

Paddison, P.J., A.A. Caudy, E. Bernstein, G.J. Hannon, and D.S. Conklin. 2002. Short hairpin RNAs (shRNAs) induce sequence-specific silencing in mammalian cells. *Genes Dev.* 16:948–958.

Pierrat, B., M. Simonen, M. Cueto, J. Mestan, P. Ferrigno, and J. Heim. 2001. SH3GLB, a new endophilin-related protein family featuring an SH3 domain. *Genomics.* 71:222–234.

Praefcke, G.J.K., and H.T. McMahon. 2004. The dynamin superfamily: universal membrane tubulation and fission molecules? *Nat. Rev. Mol. Cell Biol.* 5:133–147.

Schmidt, A., and W.B. Huttner. 1998. Biogenesis of synaptic-like microvesicles in perforated PC12 cells. *Methods.* 16:160–169.

Schmidt, A., M. Wolde, C. Thiele, W. Fest, H. Kratzin, A.V. Podtelejnikov, W. Witke, W.B. Huttner, and H.D. Soling. 1999. Endophilin I mediates synaptic vesicle formation by transfer of arachidonate to lysophosphatidic acid. *Nature.* 401:133–141.

Sever, S., H. Damke, and S.L. Schmid. 2000. Dynamin:GTP controls the formation of constricted coated pits, the rate limiting step in clathrin-mediated endocytosis. *J. Cell Biol.* 150:1137–1148.

Smirnova, E., L. Griparic, D.-L. Shurland, and A.M. van der Bliek. 2001. Dynamin-related protein Drp1 is required for mitochondrial division in mammalian cells. *Mol. Biol. Cell.* 12:2245–2256.

Weigert, R., M.G. Silletta, S. Spano, G. Turacchio, C. Cericola, A. Colanzi, S. Senatore, R. Mancini, E.V. Polishchuk, M. Salmona, et al. 1999. CtBP/BARS induces fission of Golgi membranes by acylating lysophosphatidic acid. *Nature.* 402:429–433.

Wolter, K.G., Y.T. Hsu, C.L. Smith, A. Nechushtan, X.G. Xi, and R.J. Youle. 1997. Movement of Bax from the cytosol to mitochondria during apoptosis. *J. Cell Biol.* 139:1281–1292.

Yoon, Y., K.R. Pitts, S. Dahan, and M.A. McNiven. 1998. A novel dynamin-like protein associates with cytoplasmic vesicles and tubules of the endoplasmic reticulum in mammalian cells. *J. Cell Biol.* 140:779–793.

Yoon, Y., K.R. Pitts, and M.A. McNiven. 2001. Mammalian dynamin-like protein DLP1 tubulates membranes. *Mol. Biol. Cell.* 12:2894–2905.

Yoon, Y., E.W. Krueger, B.J. Oswald, and M.A. McNiven. 2003. The mitochondrial protein hFis1 regulates mitochondrial fission in mammalian cells through an interaction with the dynamin-like protein DLP1. *Mol. Cell. Biol.* 23:5409–5420.